N_2 in a thin-walled Lindemann capillary. Precise lattice constants for a triclinic cell, determined from a least-squares fit of 15 diffractometer-measured 2θ values at 25 °C, were a = 13.444 (7) Å, b = 13.028 (7) Å, c = 16.149 (8) Å, α = 69.13 (3)°, β = 87.57 (3)°, and γ = 120.03 (3)°. The cell volume was 2201 (2) Å^3 with a calculated density of 1.266 g/cm^3. The space group was determined to be $P\bar{1}$ (Z = 1) and the absorption coefficient (μ(Cu Kα)) was 56.07 cm^{-1}. All unique diffraction maxima ($h,\pm k,\pm l$) with $\theta \leq 110.0°$ were measured on a four-circle, computer-controlled diffractometer (Syntex $P2_1$) with a variable 1° ω scan using graphite-monochromated Cu Kα radiation (1.5418 Å). After correction for Lorenz, polarization, and background, 4054 (86.2%) of the merged and averaged unique data (4702) were judged observed ($|F_o| \geq 6\sigma(F_o)$).[87] Structure solution proceeded by using the SHELXTL PLUS system. The Ta was located via Patterson synthesis and the non-hydrogen light atoms were revealed with difficulty by successive Fourier syntheses. An inspection of difference maps following refinement of the initial model revealed disorder in each of the peripheral ^{t}Bu groups. After applying several models, one in which silox-1 (Si1, O1, etc.) contained two different sets of ^{t}Bu-group conformations related by a mirror plane proved to be best. Constraints were applied to the geometries of the ^{t}Bu fragments on each silox ligand such that chemically equivalent interatomic distances were constrained to equal the same least-squares variables (e.g., all d(SiC_{tert}) are equivalent; all d($C_{tert}C$) are equivalent; all d-($C_{tert}C_{tert}$) are equivalent, etc.). At the end of the isotropic refinement, the empirical absorption correction of Walker and Stuart was applied,[88] but this proved to have little effect (0.2%) on the final structure factors. Full-matrix, least-squares refinements (minimization of $\sum w(|F_o| - |F_c|)^2$, where w is based on counting statistics modified by an ignorance factor ($w^{-1} = \sigma^2(F) + 0.03F^2$)), with anisotropic Ta, Si, O, and carbide atoms, the remaining carbons included as isotropic and all hydrogens included at calculated positions (Riding model, fixed isotropic U), have converged to R = 9.56% and R_w = 10.05%.[89] A similar refinement using all unique data (4702, excluding zeros) resulted in an R of 10.5% and an R_w of 10.1%. The fractional coordinates and thermal parameters are listed in the supplemental material.

Acknowledgment. Primary support from the Air Force Office of Scientific Research (AFOSR-87-0103) and the National Science Foundation (CHE-8714146) are gratefully acknowledged as are contributions from Chevron Research Co., the Union Carbide Innovation Recognition Program, and Cornell University. We thank Profs. David B. Collum, Barry K. Carpenter, Francis J. DiSalvo, and Klaus H. Theopold for helpful discussions and John F. Mitchell for aid in the X-ray structural studies. We also thank Dr. Bruce Chase of Du Pont Central Research for conducting the Raman experiments. Support for the Cornell NMR facility from the NIH and NSF Instrumentation Programs is acknowledged.

Registry No. 1, 102307-77-7; **2**, 104092-13-9; THF-**2**-CO, 123027-43-0; **2**-CO, 123027-44-1; **2**-$(CO)_2$, 123027-45-2; **3**, 123027-42-9; **4**, 102307-78-8; **5**, 104092-15-1; **5'**, 123027-40-7; **6**, 123027-41-8; **7**, 123051-54-7; Na(silox), 97733-16-9; CO, 630-08-0; (silox)H, 56889-90-8; PhC≡CPh, 501-65-5; ethylene, 74-85-1.

Supplementary Material Available: Honda-Owens plot of $[(silox)_3Ta]_2(\mu\text{-}C_2)$ (**5**), Curie plot of $(silox)_3$(THF)TaCO (THF-**2**-CO), tables of crystal data encompassing data collection and solution and refinement, figures showing the disorder model, tables of atomic coordinates and isotropic temperature factors, anisotropic temperature factors of core atoms, hydrogen atom coordinates, bond lengths, and bond angles for **5** (13 pages); listing of observed and calculated structure factors (17 pages). Ordering information is given on any current masthead page.

(87) Cromer, D. T.; Mann, J. B. *Acta Crystalogr., Sect. A* **1968**, *A24*, 321-324.

(88) Walker, N.; Stuart, D. *Acta Crystallogr., Sect. A* **1983**, *A39*, 158-166.

(89) $R = \sum||F_o| - |F_c||/(\sum|F_o|)$; $R_w = [\sum w(|F_o| - |F_c|)^2/\sum w(|F_o|)^2]^{1/2}$.

Vibrational Characterization of Multiply Metal-Metal Bonded Osmium, Molybdenum, and Rhenium Porphyrin Dimers

C. Drew Tait,[1a] James M. Garner,[1b] James P. Collman,*[,1b] Alfred P. Sattelberger,*[,1a] and William H. Woodruff*[,1a]

Contribution from the Inorganic and Structural Chemistry Group (INC-4), Los Alamos National Laboratory, Los Alamos, New Mexico 87545, and the Department of Chemistry, Stanford University, Stanford, California 94305. *Received May 18, 1989*

Abstract: The resonance Raman (RR) scattering and infrared (IR) absorption spectra of $\{[M(OEP)]_2\}^{n+}$ complexes [OEP = 2,3,7,8,12,13,17,18-octaethylporphyrin dianion; M = Os (n = 0-2), Re (n = 0-2), and Mo (n = 0)] are reported. Resonance Raman studies reveal the Os-Os stretch to increase in frequency upon oxidation [233 cm^{-1} (n = 0), 254 cm^{-1} (n = 1), and 266 cm^{-1} (n = 2)], consistent with the removal of electrons from π^* metal-metal antibonding orbitals. The Mo-Mo stretch was also observed spectroscopically, producing a RR peak at 341 cm^{-1}, while the Re-Re stretch in $\{[Re(OEP)]_2\}^{1+}$ was observed at 290 cm^{-1}. The corresponding metal-metal bond distances estimated from these stretching frequencies are 2.39, 2.31, and 2.27 Å for the osmium oxidation series, 2.23 Å for the molybdenum dimer, and 2.20 Å for the rhenium dimer. The porphyrin-centered vibrational modes (both RR and IR active) for the three osmium complexes are essentially independent of oxidation state, consistent with oxidation of metal-metal antibonding electrons. Little π back-bonding between the metal and porphyrin macrocycle is suggested from porphyrin RR indicator modes, which are sensitive to π electron density. Moreover, the porphyrin core size (center to nitrogen distance) is estimated from core size marker vibrations to be ca. 2.04 Å for all of the complexes studied. Finally, no vibrational evidence for ground-state intradimer coupling between the π orbitals of the porphyrin rings is found.

Detailed spectroscopic and structural investigations of binuclear transition-metal complexes containing unbridged metal-metal multiple bonds are often compromised by the failure of ancillary ligands to remain substitutionally inert when the dimers are oxidized or reduced.[2-4] Ligand lability in the redox partners fre-

(1) (a) Los Alamos National Laboratory. (b) Stanford University.

(2) Cotton, F. A.; Walton, R. A. *Multiple Bonds between Metal Atoms*; Wiley: New York, 1982.

0002-7863/89/1511-9072$01.50/0

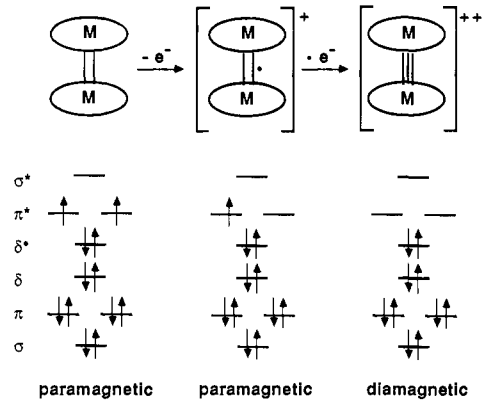

Figure 1. Oxidation-induced variations of the electronic configuration and magnetic properties in d^6 metal(II) porphyrin dimers.

quently leads to higher nuclearity clusters, bridges across the metal–metal bond, or substitutions that obscure changes in metal–metal bonding as a function of electronic configuration. Binuclear compounds incorporating the 2,3,7,8,12,13,17,18-octaethylporphyrin dianion (OEP) overcome these complications because this rigid, tetradentate, square-planar ligand is incapable of bridging two metals and its steric properties prevent the formation of higher nuclearity clusters.[5-8]

Our recent paper on the vibrational spectra of the series $\{[Ru(OEP)]_2\}^{n+}$ (n = 0–2) has shown the utility of resonance Raman (RR) spectroscopy in identifying the metal–metal stretching frequencies in porphyrin dimers and, subsequently, in estimating M–M bond force constants and lengths.[9] The observed increase in the M–M bond force constant as n increases from 0 to 1 to 2 gave further experimental verification for the metal–metal bonding scheme proposed[6,8] for the ruthenium compounds (Figure 1).[9] The ground-state electronic configuration of the neutral ruthenium(II,II) dimer is $\sigma^2\pi^4\delta^2\delta^{*2}\pi^{*2}$, resulting in a formal bond order of 2. Successive oxidations remove the two π^* electrons, increasing the bond order to 2.5 and 3. The electrochemical, magnetic, and optical properties of the three dimers are also consistent with this bonding scheme.[8]

Herein we report the vibrational spectra of the analogous $\{[Os(OEP)]_2\}^{n+}$ series (n = 0–2). Resonance Raman spectra of *unbridged* multiply metal–metal bonded diosmium complexes have not been reported previously.[10] Clark and co-workers[11] described the resonance Raman spectra of the carboxylate-bridged diosmium(III,III) complexes $Os_2(O_2CCH_3)_4Cl_2$[12] and $Os_2(O_2CCD_3)_4Cl_2$, both with a bond order of 3, so that comparisons to the osmium porphyrin dimers can be made. Other complexes studied here include $\{[Mo(OEP)]_2\}^0$ and $\{[Re(OEP)]_2\}^{n+}$ (n = 0–2).

The porphyrin-based vibrations of the preceding complexes also have been studied, both by RR and infrared (IR) absorption. The vast literature of porphyrin RR spectra allows empirical correlations to be made between porphyrin structural parameters and vibrational frequencies.[13,14] Previous work on the ruthenium porphyrin dimers has shown that these correlations can be extended to the dimeric species.[9] Information such as the extent of π back-bonding and the porphyrin core size can be extracted from the vibrational data. In addition to this porphyrin structural information, the porphyrin-based vibrations can be used to determine the extent of π-system overlap in the ground state of the two macrocycles, which are held together cofacially at <4 Å average distance.[6,15] This type of overlap has been identified in some porphyrin and phthalocyanine π-system aggregates.[16] After treatment of the metal–metal stretching frequencies, these porphyrin-based modes will be discussed.

Experimental Section

The air-sensitive neutral osmium,[5] molybdenum,[5,6] and rhenium[17] porphyrin dimers were prepared and purified as previously described. Stoichiometric amounts of $AgBF_4$ were added to the neutral osmium and rhenium dimers to produce the one- and two-electron oxidation products.[8,17] Tetrahydrofuran (THF) and toluene were distilled from Na/K alloy and stored in a Vacuum Atmospheres inert atmosphere glovebox equipped with a high-capacity gas purification system (MO-40). The neutral dimers are unstable in chlorinated solvents and in strongly coordinating solvents, so THF was chosen for the Raman experiments. While the monocation dimers are soluble in THF, the dication dimers are not. Fortunately, the cationic dimers are soluble and stable in chlorinated solvents, allowing the use of methylene chloride and chloroform-*d*, both of which contain fewer obscuring solvent vibrational bands than THF. The chlorinated solvents were dried with P_4O_{10}, distilled, and stored in the glovebox. RR samples prepared in the glovebox were sealed with a Teflon vacuum stopcock, removed from the box, subjected to a freeze–pump–thaw cycle, and flame sealed. IR samples prepared in the glovebox were sealed in KBr or NaCl cavity cells (0.1-mm path length) equipped with a vacuum-tight Teflon stopper and holder (Spectra-Tech).

Excitation for the RR experiments was provided by Ar^+ and Kr^+ ion lasers (Spectra Physics Models 171 and 2025). To minimize photodecomposition, samples were cooled to ca. −10 °C with a circulating antifreeze bath, and the laser power was reduced to 10 mW when exciting into the Soret and 30 mW elsewhere. The excitation was line-focused to reduce further the power density at the sample. Scattered light was focused into either a SPEX or an Instruments SA/Jobin Yvon scanning double monochromator (slits set to 3–5-cm^{-1} resolution; frequency precision for strong peaks ±2 cm^{-1}). Because the precision of the depolarization ratios (ρ) obtained was only ±0.1, only general information such as whether bands were polarized (a_{1g} modes) could be determined. Any z component (i.e., along the M–M axis) to the absorption giving rise to the resonant enhancement could not be inferred from deviation of ρ from 0.125 for the symmetric modes.[15c]

Infrared absorption measurements were performed with a Digilab FTS-40 FTIR at 2-cm^{-1} resolution, employing triangular apodization, and signal averaging over 1920 scans.

(3) *Inorganic Chemistry: Toward the 21st Century*; Chisholm, M. H., Ed.; ACS Symposium Series 211; American Chemical Society: Washington, DC, 1983.
(4) Recent Advances in the Chemistry of Metal–Metal Multiple Bonds. Chisholm, M. H., Ed. *Polyhedron* Symposia-in-Print No. 4, **1987**, *6*, 667–801.
(5) Collman, J. P.; Barnes, C. E.; Woo, L. K. *Proc. Natl. Acad. Sci. U.S.A.* **1983**, *80*, 7684–7688.
(6) Collman, J. P.; Barnes, C. E.; Swepston, P. N.; Ibers, J. A. *J. Am. Chem. Soc.* **1984**, *106*, 3500–3510.
(7) Collman, J. P.; Woo, L. K. *Proc. Natl. Acad. Sci. U.S.A.* **1984**, *81*, 2592–2596.
(8) Collman, J. P.; Prodolliet, J. W.; Leidner, C. R. *J. Am. Chem. Soc.* **1986**, *108*, 2916–2921.
(9) Tait, C. D.; Garner, J. M.; Collman, J. P.; Sattelberger, A. P.; Woodruff, W. H. *J. Am. Chem. Soc.*, in press.
(10) (a) The only other known unbridged multiply bonded diosmium complexes are the octahalodiosmate(III) anions $Os_2X_8^{2-}$ (X = Cl or Br).[10b,c] (b) Fanwick, P. E.; King, M. K.; Tetrick, S. M.; Walton, R. A. *J. Am. Chem. Soc.* **1985**, *107*, 5009–5011. (c) Agaskar, P. A.; Cotton, F. A.; Dunbar, K. R.; Falvello, L. R.; Tetrick, S. M.; Walton, R. A. *J. Am. Chem. Soc.* **1986**, *108*, 4850–4855.
(11) Clark, R. J. H.; Hempleman, A. J.; Tocher, D. A. *J. Am. Chem. Soc.* **1988**, *110*, 5968–5972.
(12) Behling, T.; Wilkinson, G.; Stephenson, T. A.; Tocher, D. A.; Walkinshaw, M. D. *J. Chem. Soc., Dalton Trans.* **1983**, 2109–2116.
(13) Back-bonding indicator modes: (a) Spiro, T. G. In *Iron Porphyrins*; Lever, A. B. P., Gray, H. B., Eds.; Addison-Wesley: Reading, MA, 1983; Part 2, pp 89–159. (b) Kitagawa, T. In *Spectroscopy of Biological Systems*; Clark, R. J. H., Hester, R. E., Eds.; Wiley: London, 1986; Vol. 13, pp 443–481, and references therein. (c) Boldt, N. J.; Goodwill, K. E.; Bocian, D. F. *Inorg. Chem.* **1988**, *27*, 1188–1191.
(14) Core size markers: (a) Felton, R. H.; Yu, N. T.; O'Shea, D. C.; Shelnutt, J. A. *J. Am. Chem. Soc.* **1974**, *90*, 3675–3676. (b) Spaulding, L. D.; Chang, C. C.; Yu, N. T.; Felton, R. H. *J. Am. Chem. Soc.* **1975**, *97*, 2517–2525. (c) Woodruff, W. H.; Kessler, R. J.; Ferris, N. S.; Dallinger, R. F.; Carter, K. R.; Antalis, T. M.; Palmer, G. In *Electrochemical and Spectrochemical Studies of Biologic Redox Components*; Kadish, K. M., Ed.; ACS Symposium Series 201; American Chemical Society; Washington, DC, 1982; Chapter 26. (d) Oertling, W. A.; Salehi, A.; Chang, C. K.; Babcock, G. T. *J. Phys. Chem.* **1987**, *91*, 3114–3116. (e) Oertling, W. A.; Salehi, A.; Chung, Y. C.; Leroi, G. E.; Chang, C. K.; Babcock, G. T. *J. Phys. Chem.* **1987**, *91*, 5887–5898.
(15) Overlap of porphyrin π systems: (a) Adar, F.; Srivastava, T. S. *Proc. Natl. Acad. Sci. U.S.A.* **1975**, *72*, 4419–4424. (b) Burke, J. M.; Kincaid, J. R.; Spiro, T. G. *J. Am. Chem. Soc.* **1978**, *100*, 6077–6083. (c) Schick, G. A.; Bocian, D. F. *J. Am. Chem. Soc.* **1983**, *105*, 1830–1838. (d) Hofmann, J. A.; Bocian, D. F. *J. Phys. Chem.* **1984**, *88*, 1472–1479. (e) Shelnutt, J. A.; Dobry, M. M.; Satterlee, J. D. *J. Phys. Chem.* **1984**, *88*, 4980–4987. (f) Shelnutt, J. A. *J. Phys. Chem.* **1984**, *88*, 4988–4992.
(16) Hoffman, B. M.; Ibers, J. A. *Acc. Chem. Res.* **1983**, *16*, 15–21.
(17) Collman, J. P.; Garner, J. M.; Woo, L. K. *J. Am. Chem. Soc.*, in press.

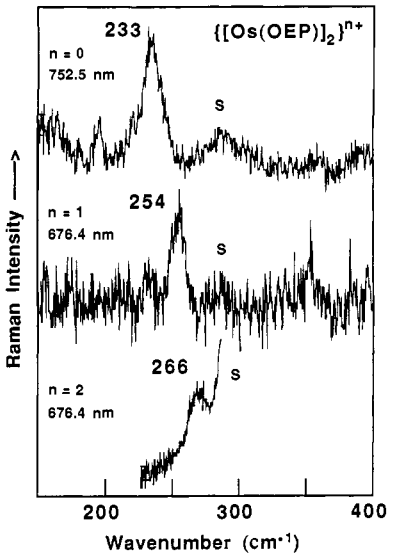

Figure 2. Resonance Raman spectra obtained from exciting the osmium porphyrin dimers in the long-wavelength region of the visible absorption spectrum. The number of electrons (n) removed from the neutral parent species and the excitation wavelength are indicated for each spectrum.

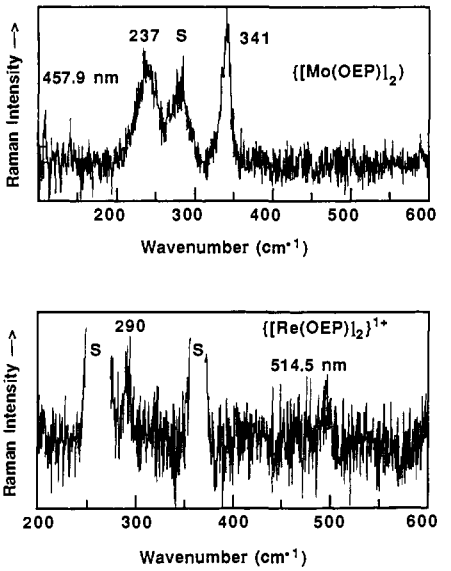

Figure 3. Low-frequency resonance Raman spectra for the molybdenum porphyrin dimer in THF and for the rhenium porphyrin monocation dimer in $CDCl_3$. The excitation wavelengths are indicated for each spectrum.

Results and Discussion

The valence shell of the neutral osmium(II,II) porphyrin dimer, like its ruthenium analogue, contains 12 electrons ($2 \times 4d^6$ for the ruthenium dimer and $2 \times 5d^6$ for the osmium dimer). Based on the proposed metal–metal bonding scheme (Figure 1), the HOMO of the paramagnetic osmium(II,II) compound is a degenerate π^* metal-centered orbital containing two electrons and the formal M–M bond order is 2.[8] Sequential one-electron chemical (e.g., with Ag^+) or electrochemical oxidation of the neutral dimer removes these antibonding electrons and the resultant paramagnetic osmium(II,III) and diamagnetic osmium(III,III) dimers have M–M bond orders of 2.5 and 3, respectively. The $E_{1/2}$ values (vs Ag/AgCl in $TBAClO_4/CH_2Cl_2$) for the metal-centered oxidations $\{[Os(OEP)]_2\}^0 - e \rightarrow \{[Os(OEP)]_2\}^{1+}$ and $\{[Os(OEP)]_2\}^{1+} - e \rightarrow \{[Os(OEP)]_2\}^{2+}$ are −0.77 and −0.01 V, respectively. The same couples for the ruthenium OEP dimers are −0.46 and +0.50, respectively.[8] As in the case of the ruthenium porphyrin dimers, non-porphyrin-based absorption bands occur in the low-energy region (>600 nm) of the visible spectrum.[5,8] Although these electronic transitions have not been assigned, they presumably contain some metal orbital contribution.[5] Excitation into this region produces the polarized resonance Raman peaks shown in Figure 2. These peaks are *not* porphyrin-based and are assigned as the Os–Os stretch for each complex. Consistent with the proposed bonding scheme, the peak frequency increases upon oxidation [233 cm^{-1} ($n = 0$) → 254 cm^{-1} ($n = 1$) → 266 cm^{-1} ($n = 2$)].

A comparison of the Os^{III}–Os^{III} stretch found for $\{[Os(OEP)]_2\}^{2+}$ (266 cm^{-1}) with that found for $Os_2(O_2CCH_3)_4Cl_2$ (229 cm^{-1})[11] might lead one to believe that the metal–metal triple bond in the porphyrin dimer is significantly stronger. However, as noted by Clark and co-workers,[11] the axial Os–Cl stretch (292 cm^{-1}) of $Os_2(O_2CCH_3)_4Cl_2$ is also a totally symmetric internal mode that is expected to couple with the Os–Os stretch. The resulting Fermi resonance will *lower* ν(Os–Os) and *raise* ν(Os–Cl) from their expected frequencies as uncoupled oscillators. Even though the "true" value of ν(Os–Os) for $Os_2(O_2CCH_3)_4Cl_2$ is unknown, we might expect it to be somewhat lower than 266 cm^{-1} because the ground-state electronic configuration[11] of paramagnetic $Os_2(O_2CMe)_4Cl_2$ is $\sigma^2\pi^4\delta^2\delta^{*1}\pi^{*1}$ (vs $\sigma^2\pi^4\delta^2\delta^{*2}$ for diamagnetic $\{[Os(OEP)]_2\}^{2+}$).

The valence shell of the neutral molybdenum(II,II) porphyrin dimer contains eight d electrons and the formation of a quadruple metal–metal bond is expected.[2-5,7] Unlike the ruthenium and osmium porphyrin dimers, no new absorption bands appear in the red region of the electronic absorption spectrum. However, a new non-porphyrin-based absorption appears in the blue region of the spectrum (437 nm),[5] and excitation at 457.9 nm produces the resonance Raman spectrum shown in Figure 3. The peak at 341 cm^{-1} is assigned as the Mo–Mo stretch and its frequency is approximately that expected based on vibrational studies of other quadruply bonded dimolybdenum(II,II) compounds (i.e., between 339 and 406 cm^{-1}).[18] We note that the polarized porphyrin-based ν_8 also should appear in the same frequency region.[19] The 341-cm^{-1} peak shown in Figure 3 is not attributed to this vibration, primarily because the excitation wavelength is between the Soret (383-nm) and Q-band (533-nm) regions and other porphyrin bands that should be enhanced with comparable intensity to ν_8 (e.g., $2\nu_{35}$ at ca. 365 cm^{-1} and $\nu_{34} + \nu_{35}$ at ca. 420 cm^{-1}) are not observed.[19]

The valence shell of the neutral rhenium(II,II) porphyrin dimer contains ten d electrons ($\sigma^2\pi^4\delta^2\delta^{*2}$) and the formation of a triple metal–metal bond is expected.[17] Despite repeated attempts to detect the Re–Re stretch of $\{[Re(OEP)]_2\}^0$ through excitation (647.1 and 676.4 nm) into the non-porphyrin-based absorptions at 622 and 646 nm,[17] no Raman peak could be detected between 200 and 350 cm^{-1}. Excitation at 514.5 nm of the monooxidized complex produced a weak peak at 290 cm^{-1} (Figure 3). No porphyrin-based vibrations were enhanced in the low-frequency region, and this frequency is in the range expected for Re–Re

Table I. Calculated Structural Parameters from Observed M–M Stretching Frequencies

	ν(M–M), cm^{-1}	k, mdyn/Å	D,[a] Å	d^n/M_2[b] (bond order)	
$\{[Ru(OEP)]_2\}^0$	285	2.42	2.39	12	(2)
$\{[Ru(OEP)]_2\}^{1+}$	301	2.70	2.33	11	(2.5)
$\{[Ru(OEP)]_2\}^{2+}$	310	2.86	2.30	10	(3)
$\{[Os(OEP)]_2\}^0$	233	2.94	2.39	12	(2)
$\{[Os(OEP)]_2\}^{1+}$	254	3.46	2.31	11	(2.5)
$\{[Os(OEP)]_2\}^{2+}$	266	3.79	2.27	10	(3)
$\{[Mo(OEP)]_2\}^0$	341	3.29	2.23	8	(4)
$\{[Re(OEP)]_2\}^{1+}$	290	4.61	2.20	9	(3.5)

[a] The bond lengths (D) are estimated from empirical relationships (ref 22). [b] d^n = total number of valence d electrons per dinuclear unit.

(18) (a) San Filippo, J., Jr.; Sniadoch, H. J. *Inorg. Chem.* **1973**, *12*, 2326–2333. (b) Clark, R. J. H.; Franks, M. L. *J. Am. Chem. Soc.* **1975**, *97*, 2691–2697. (c) Reference 2, pp 425–432.

(19) (a) Kitagawa, T.; Abe, M.; Ogoshi, H. *J. Chem. Phys.* **1978**, *69*, 4516–4525. (b) *Ibid.* 4526–4534.

stretches (e.g., 275–318 cm^{-1} for the octahalodirhenates $Re_2X_8^{2-}$, X = F, Cl, Br).[20] Therefore, the 290-cm^{-1} peak is tentatively assigned as the Re–Re stretch in $\{[Re(OEP)]_2\}^{1+}$. A weak peak at ca. 286 cm^{-1} (not shown) was observed in the Raman spectrum of $\{[Re(OEP)]_2\}^{2+}$ and is tentatively assigned as the quadruple Re–Re bond stretching vibration.

Table I lists the frequencies for the metal–metal stretches that have been assigned in this study and in the previous ruthenium porphyrin dimer study.[9] Comparisons between the metal–metal force constants for the different metals can be made, where the force constants are estimated by using the diatomic approximation to the stretch.[21] Although their valence shells have the same number of electrons and hence the same bond order, each osmium porphyrin dimer has a larger force constant than the corresponding ruthenium porphyrin dimer. In fact, the force constant of triply bonded $\{[Ru(OEP)]_2\}^{2+}$ is *smaller* than the force constant of doubly bonded $\{[Os(OEP)]_2\}^{0}$. This result indicates that the 5d orbitals of osmium form stronger metal–metal bonds than the 4d orbitals of ruthenium, presumably because of greater orbital overlap. This trend may explain why iron porphyrin dimers have not been made despite repeated attempts.[5] Consider now the estimated force constant for the Mo–Mo stretch of $\{[Mo(OEP)]_2\}$. This quadruple bond is composed of 4d orbitals, and although its force constant is greater than any of the Ru–Ru force constants, the Mo–Mo bond strength is comparable to that of an osmium porphyrin dimer with a bond order between 2 and 2.5. Finally, the force constant for $\{[Re(OEP)]_2\}^{1+}$ is the largest we have found, consistent with a bond order of 3.5 and effective 5d orbital overlap.

Bond distances between the metals in the porphyrin dimers may also be estimated from empirical force constant/bond distance relationships.[22] The estimated metal–metal separations for the ruthenium, osmium, molybdenum, and rhenium porphyrin dimers are also listed in Table I. The predicted bond distance in the neutral ruthenium porphyrin dimer (2.39 Å) is in excellent agreement with the value obtained from X-ray crystallography (2.41 Å).[6,9] In addition, the estimated Os–Os bond distance in the diosmium(III,III) complex (2.27 Å) is close to that found in the X-ray crystal structure for $Os_2(O_2CCH_3)_4Cl_2$ (2.31 Å).[23] The similarity between the bond distances predicted for the ruthenium dimers and the corresponding osmium dimers is striking but consistent with almost identical atomic radii tabulated for higher oxidation states of these metals.[24]

The estimated Mo–Mo distance in $\{[Mo(OEP)]_2\}^{0}$ (2.23 Å) is comparable to that found (X-ray) for the related molybdenum(II) tetraphenylporphyrin (TPP) dimer (2.24 Å).[25] However, it is significantly longer than the Mo–Mo bond distances in the $Mo_2X_4(PMe_3)_4$ compounds (~2.13 Å; X = Cl, Br, I).[26] It is not unreasonable to suggest that the increase in Mo–Mo bond lengths from the halo–phosphine dimers to the porphyrin systems is, at least partially, a reflection of porphyrin–porphyrin repulsion. The previously observed low-temperature (−45 °C) coalescence of the 300-MHz ^1H NMR signals of meso-substituted molybdenum porphyrin dimers indicates a dynamic rotation of porphyrin groups about the Mo–Mo bond.[7] While the σ and π bonds are both cylindrically symmetric about the metal–metal axis, the δ bond is not. Because maximum δ overlap occurs in the rigorously eclipsed conformation (D_{4h} symmetry),[7] this rotation would decrease the contribution of the δ bond at rotational angles other than rigorously eclipsed, giving rise to a continuous spread of Mo–Mo stretching frequencies corresponding to different conformations, and different δ-bond contributions. While such an effect, if observed, might yield information concerning the δ contribution to overall bond strength, no such broadening is noted in the present case. The most likely explanation for this is that the conformational populations are Boltzmann weighted, strongly favoring nearly eclipsed conformations near the energy minimum represented by maximum δ overlap.

Finally, the estimated Re–Re bond length of $\{[Re(OEP)]_2\}^{1+}$ (2.20 Å) can be compared to that found in the octahalodirhenates $Re_2X_8^{2-}$ (X = F, 2.20 Å; X = Cl, 2.22 Å; X = Br, 2.23 Å)[27,28] and in $\{Re_2Cl_4(PMe_2Ph)_4\}^{1+}$ (2.22 Å).[29,30] Note that the metal–metal bond order of the cationic porphyrin and phosphine dimers (3.5) is less than that of the octahalide dimers (4.0). Removal of the final δ^* electron appears to have little effect on the bond length.[30] If the Re–Re stretch of $[[RenOEP)]_2]^{2+}$ is indeed at 286 cm^{-1}, the bond length actually is predicted to increase to 2.21 Å, despite an increase in the formal bond order. However, the competing effect of orbital contraction upon oxidation on the overlap of the stronger σ and π bonds must also be considered. Such a competing effect has been invoked previously to explain minimal changes in Re–Re bond distance [$\{Re_2Cl_4(PMe_3)_4\}^{1+}$ (2.218 Å) → $\{Re_2Cl_4(PMe_3)_4\}^{2+}$ (2.215 Å)] and an actual *increase* in Tc–Tc bond distance [$Tc_2Cl_8^{3-}$ (2.117 Å) → $Tc_2Cl_8^{2-}$ (2.151 Å)] upon oxidation and concomitant increase in bond order from 3.5 to 4.0.[29,31] This is taken as further evidence that larger orbitals with greater overlap form the stronger metal–metal bonds.

Excitation into the porphyrin-based Soret and Q bands of the dimeric complexes produces resonance Raman scattering from the porphyrinic vibrations. As in the ruthenium porphyrin dimers, these vibrations can be assigned, to a first approximation, according to the corresponding OEP monomer vibrations (Table II).[9,19] Assignments were determined from peak positions and depolarization ratios. Polarized peaks are associated with a_{1g} modes, depolarized peaks with either b_{1g} or b_{2g} modes, and anomalously polarized peaks with a_{2g} modes.[32]

The porphyrin-based vibrations can be used to investigate the bonding between the metal center and the porphyrin macrocycle. Specifically, mode ν_4 is associated with electron density in the porphyrin π system and hence is affected by the extent of π back-bonding.[13] Sensitivity to π back-bonding has also been attributed to ν_{11}.[13c] The presence of π back-bonding will add electron density to the porphyrin antibonding π system and result in weaker bonds and in the appearance of ν_4 and ν_{11} in the lower frequency region of their respective ranges. Conversely, negligible π back-bonding will result in the appearance of ν_4 and ν_{11} in the higher frequency region of their respective ranges.

Of the metals studied here, osmium(II) is undoubtedly the best π back-bonder. In monomeric osmium(II) porphyrin compounds, the osmium has been shown to back-bond equatorially to the

(20) (a) Clark, R. J. H.; Franks, M. L. *J. Am. Chem. Soc.* **1976**, *98*, 2763–2767. (b) Clark, R. J. H.; Stead, M. H. In *Inorganic Chemistry: Toward the 21st Century*; Chisholm, M. H., Ed.; ACS Symposium Series 211; American Chemical Society: Washington, DC, 1983; pp 235–240. (c) Morris, D. E.; Tait, C. D.; Dyer, R. B.; Schoonover, J. R.; Hopkins, M. D.; Sattelberger, A. P.; Woodruff, W. H. *Inorg. Chem.*, in press.

(21) $k = (3.55 \times 10^{17})\mu\nu^2$, where k is the force constant (in mdyn/Å), μ the reduced mass of the two metal atoms (in g), and ν the vibrational frequency (in cm^{-1}).

(22) Miskowski, V. M.; Dallinger, R. F.; Christoph, G. G.; Morris, D. E.; Spies, G. H.; Woodruff, W. H. *Inorg. Chem.* **1987**, *26*, 2127–2132. The appropriate equation for elements Rb–Xe is $r = 1.83 + 1.51 \exp(-k/2.48)$; and for elements Cs–Rn is $r = 2.01 + 1.31 \exp(-k/2.36)$, where r is in Å and k is in mdyn/Å.

(23) Cotton, F. A.; Chakravarty, A. R.; Tocher, D. A.; Stephenson, T. A. *Inorg. Chim. Acta* **1984**, *87*, 115–119.

(24) Huheey, J. E. *Inorganic Chemistry: Principles of Structure and Reactivity*, 2nd ed.; Harper and Row Publishers: New York, 1978; pp 71–74.

(25) Yang, C. H.; Dzugan, S. J.; Goedken, V. L. *J. Chem. Soc., Chem. Commun.* **1986**, 1313–1315.

(26) (a) Cotton, F. A.; Extine, M. W.; Felthouse, T. R.; Kolthammer, B. W. S.; Lay, D. G. *J. Am. Chem. Soc.* **1981**, *103*, 4040–4045. (b) Hopkins, M. D.; Schaefer, W. P.; Bronikowski, M. J.; Woodruff, W. H.; Miskowski, V. M.; Dallinger, R. F.; Gray, H. B. *J. Am. Chem. Soc.* **1987**, *109*, 408–416.

(27) (a) Cotton, F. A.; Frenz, B. A.; Stults, B. R.; Webb, T. R. *J. Am. Chem. Soc.* **1976**, *98*, 2768–2773. (b) Huang, H. W.; Martin, D. S. *Inorg. Chem.* **1985**, *24*, 96–101.

(28) Conradson, S. D.; Sattelberger, A. P.; Woodruff, W. H. *J. Am. Chem. Soc.* **1988**, *110*, 1309–1311.

(29) Cotton, F. A.; Dunbar, K. R.; Falvello, L. R.; Tomas, M.; Walton, R. A. *J. Am. Chem. Soc.* **1983**, *105*, 4950–4954.

(30) Bursten, B. E.; Cotton, F. A.; Fanwick, P. E.; Stanley, G. G.; Walton, R. A. *J. Am. Chem. Soc.* **1983**, *105*, 2606–2611.

(31) (a) Cotton, F. A.; Daniels, L.; Davison, A.; Orvig, C. *Inorg. Chem.* **1981**, *20*, 3051–3055. (b) Cotton, F. A.; Davison, A.; Day, V. W.; Fredrich, M. F.; Orvig, C.; Swanson, R. *Inorg. Chem.* **1982**, *21*, 1211–1214.

(32) Bernstein, H. J. *Philos. Trans. R. Soc. London, A* **1979**, *293*, 287–302.

Table II. Porphyrin RR Vibrational Assignments for $\{[M(OEP)]_2\}^{n+}$ [a]

Os			Re			Mo		
$n = 0$	1	2	0	1	2	0		
2[b]	2.5	3	3	3.5	4	4	assignment[c]	
1032	1032		1027	1029	1032	1028	ν_5	a_{1g}
1067					(1059)	(1059)		
	1127			1125		(1130)	(ν_{22}	a_2g)
1149	1146	1151	1146	1142	(1141)	1141	(ν_{14}	b_{1g}
1154				1154	1149		and/or	
							$\nu_6 + \nu_8$	a_{1g})
1167							(ν_{30}	b_{2g})
1219	1215	1221	1215	1217	1220	1212	ν_{13}	b_{1g}
1257			1257	1260	(1260)	1257	$\nu_5 + \nu_9$	a_{1g}
1321	1316	1307	1318	1310	1305	1316	ν_{21}	a_{2g}
					1355	1361	ν_{12}	b_{1g}
1374	1378	1382	1379	1372	1371	1371	ν_4	a_{1g}
1387					1382	1385	ν_{20}	a_{2g}
1407	1408	1417	1406	1407	1407	1395	ν_{29}	b_{2g}
				(1440)				
1464			1461	1459	1469	1462	(ν_{28}	b_{2g})
1485	1485		1491	1494	1493	1485	ν_3	a_{1g}
		1538		1536		1532		
1553	1554	1557	1552	1552	1549	1554	ν_{11}	b_{1g}
1565					1569	1570	ν_{19}	a_{2g}
1578	1578	1577	1575	1577	(1583)		ν_2	a_{1g}
1614			1626	1629	1634	1602	ν_{10}	b_{1g}

[a] Solvents used: $n = 0$, THF; $n = 1$, THF, CH_2Cl_2, $CDCl_3$; $n = 2$, CH_2Cl_2, $CDCl_3$. [b] Metal–metal bond order. [c] Assignments in parentheses are tentative due to lack of intensity, and, hence, lack of depolarization ratio. Vibrational band numbering corresponds to that in ref 9 and 19.

Table III. IR Frequencies of Cationic Porphyrin Dimers in CH_2Cl_2[a]

Ru			Re		Os			
monomer[b]	1	2	1	2	1	2	assignments[c]	
830		824					$\pi(C_mH)$	
847	854	854	851	858	856	862	$\pi(C_mH)$	
921	922	922	922	925	925	927	ν_{46}	$\{\nu(C_\alpha Cm), \nu(C_\beta C_s)\}$
960	961	960	963	965	964	965		ethyl group
991	992	992	990	989	995	996	ν_{45}	$\{\nu(C_\alpha N), \nu(C_\alpha C_m)\}$
1019	1017	1017	1019	1021	1021	1022		ethyl group
	1038	1038	1038	1038	1038	1038		BF_4^-
1058	1056	1056	1057	1055	1056	1055		ethyl group
1064								ethyl group
	1094	1094		1092	1094	1094		BF_4^-
1110	1112	1110	1111	1110	1112	1113		ethyl group
	1125		1126				ν_{44}	$\{\nu(C_\alpha N), \delta(C_\alpha C_m H)\}$
1149	1148	1148	1150	1150	1150	1150	ν_{43}	$\{\nu(C_\alpha N), \delta(C_\alpha C_m H)\}$
1229	1221		1221				ν_{42}	$\{\nu(C_\alpha N), \delta(C_\alpha C_m H)\}$
S	1272	1272	1271		1271	1271	ν_{41}	$\{\nu(C_\alpha C_\beta), \nu(C_\beta C_\beta)\}$
1305	1294	1287	1285	1289	1286	1286		
1317	1317	1314		1320				ethyl group
1365	1363	1362	1367	1359	1368	1366		
1379	1378	1378	1377	1379	1377	1381		ethyl group
	1390	1391	1389	1392	1397	1399	ν_{40}	$\{\nu(C_\alpha C_\beta), \nu(C_\beta C_s)\}$
1453	1453	1453	1452	1454	1452	1453		ethyl group
1467	1467	1467	1466	1467	1466	1467		ethyl group
	1480		1474	1477				
	1499	1501	1491	1495	1490	1491	ν_{39}	$\nu(C_\alpha C_m)$
1538	1522			1527	1533	1532		
1551	1554	1553	1552	1553	1552	1552	ν_{38}	$\nu(C_\alpha C_m)$
1600	1594			1589	1593	1593	ν_{37}	$\nu(C_\beta C_\beta)$

[a] Abbreviations: C_α, C_β, C_m, C_s, porphyrin α, β, methine, and substituent (ethyl) carbons, respectively, S, solvent; ν, stretch; δ, in-plane bend; π, out-of-plane bend. [b] Ru(OEP)(CO), ref 9. [c] See ref 35.

porphyrin macrocycle in the absence of a π-accepting axial ligand.[13c,33] Loss of equatorial π back-bonding to the porphyrin has been studied in osmium(II) porphyrins with axial carbonyl ligands. The latter ligand accepts Os(II) $d\pi$ electron density. With this substitution, e.g., going from Os(OEP)py_2 to Os(OEP)(CO)py, ν_4 was observed to shift by +9 cm^{-1} (1365 → 1374 cm^{-1}) consistent with diminution of equatorial back-bonding.[13c] In addition, ν_{11} was observed to shift by +23 cm^{-1} (1523 → 1546 cm^{-1}) from the bis(pyridine) complex to the (CO)py adduct.[13c]

From Table II, we see that ν_4 and ν_{11} for *all* of the osmium dimers are at the high wavenumber ends of the ν_4 and ν_{11} ranges. This leads to the conclusion that there is only weak π back-bonding to the porphyrins in all three osmium dimers.

At least two explanations for the reduction of π back-bonding in the dimer systems can be advanced. First, we note that both porphyrinato cores of the structurally characterized $\{(Ru(OEP)_2\}^0$ (and, presumably, the porphyrinato cores of all of the OEP dimers) have domed-type distortions.[6] It is not unreasonable to suggest that this metal–porphyrin orientation results in unfavorable overlap between the metal $d\pi^*$ orbitals and the porphyrin π^* orbitals. A second consideration is based on the observation that the metal dimer π^* orbitals, from which electrons would be donated via π

(33) (a) Antipas, A.; Buchler, J. W.; Gouterman, M.; Smith, P. D. *J. Am. Chem. Soc.* **1978**, *100*, 3015–3024. (b) Antipas, A.; Buchler, J. W.; Gouterman, M.; Smith, P. D. *J. Am. Chem. Soc.* **1980**, *102*, 198–207.

back-bonding, are at most only half-filled (see Figure 1). This is in contrast to the monomeric porphyrins, where the metal π-bonding orbitals (d_{xz}, d_{yz}) are filled for Os(II). The reduction of $d\pi$ density in the dimer must reduce equatorial back-bonding. Note that this redistribution of electron density is a direct result of M–M bonding, since the unfilled d_{z^2} orbitals in the monomer combine to form a σ metal–metal bonding orbital in the dimer that must be filled with two electrons before the $d\pi^*$ orbitals.

The highest frequency anomalously polarized mode, ν_{19} (a_{2g}), has been correlated to core size of the porphyrin macrocycle.[14] Our previous study of ruthenium porphyrin dimers suggests that such a correlation can be extended to this class of dimeric systems.[9] From Table II, we see that the ν_{19} modes found vary over a small range (1565–1570 cm^{-1}), indicating a porphyrin center to nitrogen distance of ca. 2.04 ± 0.01 Å, identical with that of the ruthenium porphyrin dimers. This distance appears to be independent of metal and metal charge and may be determined primarily by the dimeric nature of the complexes. If, as expected, the structures of these dimers are similar to that of $[Ru(OEP)]_2$,[6] each metal is displaced well out of the porphyrin nitrogen plane toward the other metal, and this undoubtedly lessens their influence on the porphyrin core size.

The porphyrin-based vibrational bands can also be used to search for evidence of porphyrin π-system overlap in the ground state. Such π overlap would be expected to lift the degeneracy of the in-phase and out-of-phase combinations of monomer modes.[15] This might be detected by a splitting of the Raman active bands.[15a] Furthermore, with no exclusion rule in the noncentrosymmetric dimer, a mode that is Raman active in the corresponding monomer can become IR active as the out-of-phase combination in the dimer, and vice versa.[15b-d] The strength of a crossover mode (i.e., a mode active as the in-phase combination in one spectroscopy and as the out-of-phase combination in the other spectroscopy) and the frequency separation between the two phase combinations are indicative of the strength of the overlap.

The vibrational bands from Tables II and III can be compared to look for evidence for porphyrin π-system overlap in the ground state. Within the 4–5-cm^{-1} resolution of the spectrometer, no splitting of the Raman bands was noted. Moreover, a comparison of Raman bands and infrared absorption bands shows little evidence of crossover modes. Because of problems of solubility and stability, only the IR spectra of the charged species were taken. The only candidate for a crossover mode appears at ~1530 cm^{-1}. However, these peaks are weak in *both* spectroscopies (and missing entirely from the spectra of some species), contrary to what is expected for a crossover mode.[15b] The resonance Raman peaks at this frequency are attributed to traces of monomer compound present and not to any dimer mode, while the corresponding IR peaks are attributed to an overtone mode.[34,35]

Our failure to detect porphyrin π-system overlap in the ground state compliments the results found previously for the ruthenium porphyrin systems.[9] There we speculated that poor π-system overlap was a consequence of the doming of the porphyrin rings away from each other.

Summary

The increase in the Os–Os stretching mode frequency (233 → 254 → 266 cm^{-1}) as electrons are removed from the metal–metal bond of $\{[Os(OEP)]_2\}^0$ provides direct vibrational evidence for the bonding scheme previously proposed.[6,8] These are the first reported frequencies for Os–Os stretches without the complicating effects of axial ligation. Values for the Mo–Mo quadruple bond stretching frequency (341 cm^{-1}) in $\{[Mo(OEP)]_2\}^0$ and the Re–Re 3.5 bond stretching frequency (290 cm^{-1}) in $\{[Re(OEP)]_2\}^{1+}$ are also reported. Metal–metal bond distances have been estimated from these vibrational frequencies, yielding values of 2.39, 2.31, and 2.27 Å for the osmium oxidation series, 2.23 Å for the molybdenum porphyrin dimer, and 2.20 Å for the rhenium complex. The porphyrin macrocycle appears to be independent of the metal–metal centers, showing no proclivity toward π back-bonding with the metals and showing no change in core size with metal or metal charge. Finally, the porphyrins appear to be independent of one another in the ground state; no vibrational evidence for π-orbital interaction is found.

Acknowledgment. The spectroscopic work was performed at Los Alamos National Laboratory under the auspices of the U.S. Department of Energy supported by a LANL Institutional Supporting Research Grant to W.H.W., and an Office of Energy Research, Division of Chemical Sciences Grant to A.P.S. C.D.T. gratefully acknowledges the support of the Director's Fellowship Program at LANL. We also thank Professor David F. Bocian (Carnegie Mellon) and Dr. Robert J. Donohoe (LANL) for helpful discussions. The synthetic work at Stanford was supported by the National Science Foundation (CHE83-18512) and the National Institute of Health (GM 17880-15, 16). J.M.G's portion of this work is dedicated to his father, James H. Garner.

Registry No. $\{[Ru(OEP)]_2\}^0$, 54762-43-5; $\{[Ru(OEP)]_2\}^{1+}$, 101494-42-2; $\{[Ru(OEP)]_2\}^{2+}$, 101658-45-1; $\{[Os(OEP)]_2\}^0$, 89184-09-8; $\{[Os(OEP)]_2\}^{1+}$, 101494-46-6; $\{[Os(OEP)]_2\}^{2+}$, 101658-44-0; $\{[Mo(OEP)]_2\}^0$, 89198-27-6; $\{[Re(OEP)]_2\}^{1+}$, 122647-72-7.

(34) Ogoshi, H.; Masai, N.; Yoshida, Z.; Takemoto, J.; Nakamoto, K. *Bull. Chem. Soc. Jpn.* **1971**, *44*, 49–51.
(35) Kincaid, J. R.; Urban, M. W.; Watanabe, T.; Nakamoto, K. *J. Phys. Chem.* **1983**, *87*, 3096–3101.